doi:10.1016/j.jmb.2006.09.001 J. Mol. Biol. (2006) 364, 411–423

JMB

Available online at www.sciencedirect.com

ScienceDirect

ELSEVIER

Mechanism of Phosphoryl Transfer Catalyzed by Shikimate Kinase from *Mycobacterium tuberculosis*

Marcus D. Hartmann, Gleb P. Bourenkov, Attila Oberschall Nicolai Strizhov and Hans D. Bartunik*

Max Planck Unit for Structural Molecular Biology
MPG-ASMB c/o DESY
Notkestrasse 85
22603 Hamburg, Germany

The structural mechanism of the catalytic functioning of shikimate kinase from *Mycobacterium tuberculosis* was investigated on the basis of a series of high-resolution crystal structures corresponding to individual steps in the enzymatic reaction. The catalytic turnover of shikimate and ATP into the products shikimate-3-phosphate and ADP, followed by release of ADP, was studied in the crystalline environment. Based on a comparison of the structural states before initiation of the reaction and immediately after the catalytic step, we derived a structural model of the transition state that suggests that phosphoryl transfer proceeds with inversion by an in-line associative mechanism. The random sequential binding of shikimate and nucleotides is associated with domain movements. We identified a synergic mechanism by which binding of the first substrate may enhance the affinity for the second substrate.

Keywords: P-loop kinase; in-line associative phosphotransfer; transition state; kinetic crystallography; X-ray crystal structure

*Corresponding author

Introduction

The shikimate pathway converts erythrose-4-phosphate into chorismate, which is an intermediate required for the biosynthesis of aromatic amino acids and other important aromatic metabolites. The pathway is used in algae, higher plants, bacteria, fungi, and apicomplexan.[1,2] It is likely to have been an ancient eukaryotic attribute, which has been lost in many taxonomes that are now dependent on exogenous aromatic compounds.[2] In particular, the pathway is absent from mammals,[3] which makes enzymes in the pathway potential targets for the development of non-toxic antimicrobial agents, herbicides, and anti-parasitic drugs.

The genomic organization of the *aro* genes in the shikimate pathway of *Mycobacterium tuberculosis* includes one operon, *aroCKBQ*, and three isolated *aro* genes, *aroE*, *aroG* and *aroA*.[4] The *aroK* gene is essential in *M. tuberculosis*.[4] It encodes the enzyme shikimate kinase (SK, EC 2.7.1.71), which catalyzes the conversion of shikimate (SKM; Figure 1) into shikimate-3-phosphate (S3P) using adenosine triphosphate (ATP) as co-substrate. The *M. tuberculosis* shikimate kinase (MtSK) has high sequence similarity, 54%, to the *aroK*-encoded SK I in *Escherichia coli*.[5] *E. coli* has a second isozyme, SK II, encoded by *aroL*, that has a much higher affinity for shikimate than SKI and normally functions in aromatic biosynthesis in the cell.[6]

Crystal structures of shikimate kinases belonging to the SK I type were determined for a number of organisms including *E. coli*,[7] *Campylobacter jejuni*,[8] *Helicobacter pylori*[9] and *M. tuberculosis*. The available MtSK structures show the enzyme in a number of liganded states, including binary complexes of MtSK with SO_4[10] or MgADP[11] (PDB code 1L4Y), and ternary complexes of MtSK with shikimate (SKM) as one ligand and SO_4[10] (2G1K), ADP[12] (1U8A), MgADP,[13] or the ATP analogue AMPPCP[10] (1ZYU) as a second ligand. Until now, no structural information has been available on the enzyme in unliganded form and in productive liganded states. Putative structures of an "apo-MtSK" and an "MtSK·SKM" complex that were reported recently[10] in fact both contained a sulfate ion bound at the nucleotide binding site, which as it is discussed below significantly affects the enzyme conformation.

Abbreviations used: SK, shikimate kinase; MtSK, *Mycobacterium tuberculosis* SK; S3P, shikimate-3-phosphate; SB, SKM-binding; ESB, extended SB; RC, reduced core; NB, nucleotide-binding.

E-mail address of the corresponding author: Bartunik@mpghdb.desy.de

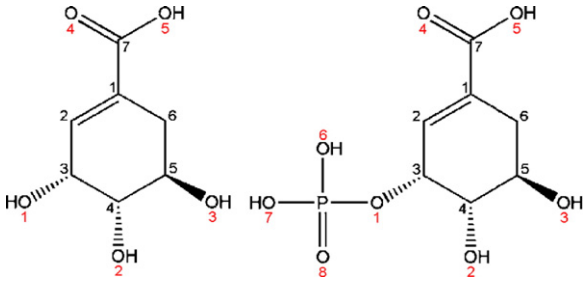

Figure 1. Atom nomenclature for SKM and S3P. The SKM nomenclature is similar to that used previously.[13] The schemes were produced with ChemDraw.

Here, we describe a number of high-resolution crystal structures of MtSK in a series of different functional states of the enzymatic reaction. These include, in particular, the (unliganded) apo-form of the enzyme, binary complexes of the enzyme with MgATP and with SKM, and a ternary complex with the products shikimate-3-phosphate (S3P) and ADP. Furthermore, we initiated catalytic turnover of shikimate and MgATP by MtSK in the crystalline environment and observed the formation of the products shikimate-3-phosphate and ADP, followed by release of ADP as the first product. On the basis of the crystal structures, which were obtained for the reaction states before initiation of the enzymatic reaction and immediately after the catalytic step, we derived a structural model of the transition state that is consistent with an in-line associative mechanism of phosphoryl transfer. Our approach is complementary to previous studies of phosphoryl transfer mechanisms in phosphokinases that utilized mimics to capture the transition state.[14]

Results and Discussion

Overall structure and domain motions

We determined crystal structures of MtSK in the apo state and in a number of different liganded states (Table 1). The structures MtSK·SO_4·SKM and MtSK·ADP·SKM are similar to the previously described structures 2G1K and 1U8A, respectively, but have substantially higher resolution. The following discussion is entirely based on the presently reported structures, except for the previously described structures MtSK·MgADP (1L4Y) and MtSK·SKM·AMPPCP (1ZYU) that are referred to by using their PDB codes.

MtSK is a member of the nucleoside monophosphate (NMP) kinase family.[15] The topology of MtSK (Figure 2) shows an α/β/α fold with a central five-stranded parallel β-sheet flanked by eight α-helices. MtSK and other NMP kinases were previously classified[7,9–13] as consisting of three domains including an SB (SKM-binding) or NMP-binding domain, a CORE domain and the LID. Based on an analysis of global movements accompanying changes in ligandation, we identified four domains in MtSK. The first domain, denoted as ESB (extended SB) domain, comprises residues 32–93. It includes the SB sub-domain (residues 32–61) that corresponds to the NMP-binding domain in NMP kinases. The second domain, constituting the nucleotide-binding (NB) site, contains the phosphate binding (P-) loop (Walker-A motif, 9–17), the AB-loop (148–155), and the segment 101–110 including α6 (104–110). The third domain is the LID (112–124). The remaining part of the molecule forms the reduced core (RC) domain. For comparison, the previously defined CORE domain comprised the present RC and NB domains plus a segment (62–93) of the ESB domain. The RC and ESB domains are nearly rigid (root-mean-square deviations of 0.5–0.6 Å for the C^{α} atoms when comparing all crystal structures). The SB sub-domain and the sub-domain comprising residues 62–93 are slightly more rigid (r.m.s. deviations of 0.4 Å and 0.3 Å, respectively) as compared to the entire ESB domain (0.55 Å). Their relative motions, however, are insignificant.

The global motions that are associated with ligandation of MtSK are described in the following with respect to the RC domain. The binding of nucleotides, ADP or ATP, induces a rotational movement of the NB domain (Figure 3(a)). This motion, which is visible, e.g. when comparing the

Table 1. Data collection and refinement statistics

Ligandation state	apo	ADP		MgATP	SKM		SKM + ADP	SKM + SO_4	S3P + SO_4	S3P + ADP
LID conformation	Open(A)	Open(A)	Open(B)	Open(B)	Open(A)	Closed	Closed	Closed	Closed	Closed
Space group	$P4_32_12$	$P4_32_12$	$P2_1$	$P2_1$	$P4_32_12$	$P1$	$P3_221$	$P3_121$	$P3_121$	$P3_121$
Resolution (Å)	1.47	1.85	1.35	1.85	1.40	1.98	1.80	1.49	1.62	2.30
Completeness (%)	97.6	98.0	97.2	98.3	95.3	96.1	97.0	99.4	93.8	95.8
Redundancy	4.05	4.67	2.51	3.54	2.90	2.20	3.08	3.04	2.31	1.96
$\langle I/\sigma(I)\rangle$	7.15	9.38	7.35	10.86	9.97	5.97	9.62	12.69	5.70	6.69
R_{merge} [a] (%)	10.0	9.0	6.6	9.8	4.5	9.5	5.9	4.3	6.4	8.8
Wilson B value	19.2	27	13.7	16.8	21.4	24.8	30.5	19.9	26.2	32.0
R_{cryst} [b] (%)	19.7	21.4	13.8	16.1	17.6	16.5	18.4	16.7	17.5	19.1
R_{free} [b] (%)	24.6	29.5	17.8	19.9	21.2	25.0	24.1	20.6	23.3	24.2
PDB code	2IYT	2IYU	2IYV	2IYW	2IYS	2IYR	2IYQ	2IYX	2IYY	2IYZ

[a] $R_{merge} = \sum|I_{obs} - \langle I\rangle| / \sum\langle I\rangle$.
[b] R factor $= \sum|F_{obs} - F_{calc}| / \sum F_{obs}$.